Journal of Mathematical Biology (2019) 78:497–526
https://doi.org/10.1007/s00285-018-1281-3

Mathematical Biology

Bone metastasis treatment modeling via optimal control

Ariel Camacho[1] · **Silvia Jerez**[1]

Received: 22 November 2017 / Revised: 29 July 2018 / Published online: 21 August 2018

Abstract
Metastatic disease is a lethal stage of cancer progression. It is characterized by the spread of aberrant cells from a primary tumor to distant tissues like the bone. Several treatments are used to deal with bone metastases formation, but they are palliative since the disease is considered incurable. Computational and mathematical models are used to understand the underlying mechanisms of how bone metastasis evolves. In this way, new therapies aiming to reduce or eliminate the metastatic burden in the bone tissue may be proposed. We present an optimal control approach to analyze some common treatments for bone metastasis. In particular, we focus on denosumab treatment, an anti-resorptive therapy, and radiotherapy treatment which has a cell killing action. We base our work in a variant of an existing model introduced by Komarova. The new model incorporates a logistic equation in order to describe the bone metastasis evolution. We provide proofs of existence and uniqueness of solutions to the corresponding optimal control problems for each treatment. Moreover, we present some numerical simulations to analyze the effectiveness of both treatments when different interactions between cancer and bone cells occur. A discussion of the obtained results is provided.

Keywords Bone metastasis · Mathematical modeling · Radiotherapy · Denosumab · Optimal control

Mathematics Subject Classification 37N25 · 34H05 · 92C30

✉ Silvia Jerez
jerez@cimat.mx

Ariel Camacho
jose.camacho@cimat.mx

[1] CIMAT, 36000 Guanajuato, Gto., Mexico

1 Introduction

The bone remodeling cycle is a continuous process in which a portion of bone tissue is eliminated by osteoclasts through a process called bone resorption, and then osteoblasts perform bone formation consisting in the deposition of newly formed bone matrix. Osteoclasts and osteoblasts are important elements of the basic multicellular unit (BMU) which carries out the bone remodeling cycle. The BMU synchronizes in an ordered way to equilibrate bone mass levels and to maintain a functional bone structure. Such coordination is rather complex and many biochemical agents and receptors take part in this process (Florencio-Silva et al. 2015).

The RANK/RANKL/OPG pathway plays a major role in the regulation of bone remodeling. This pathway is composed of the receptor activator of nuclear factor κB (RANKL), its receptor, RANK, and osteoprotegerin (OPG). Osteoblasts produce RANKL and OPG, while osteoclasts express RANK. Bone resorption is triggered when osteoclast precursors become active due to RANK–RANKL. To counteract this process, osteoblasts produce OPG which is a decoy receptor for RANKL that prevents RANK–RANKL bindings. The RANKL/OPG ratio determines in great way the BMU fate (Florencio-Silva et al. 2015).

Computational and mathematical models in the literature have been proposed to describe the dynamics of the bone remodeling process. The majority of the computational models are based on cellular automata algorithms to simulate bone structural adaptation (Tovar 2004; Penninger et al. 2008; Van Scoy et al. 2017). On the other hand, mathematical models are usually constructed via a system of differential equations that are based on the biochemical interactions between the BMU cells at a bone remodeling site (Komarova et al. 2003; Lemaire et al. 2004; Pivonka et al. 2008; Graham et al. 2012; Jerez and Chen 2015; Ross et al. 2017; Jerez et al. 2018). In the latter case, two families of differential models can be distinguished: one consisting of models at cellular and molecular scale following Lemaire work, and another with nonlinear models known as Komarova type equations where the nonlinearities are given by a power law (Savageau 1988) that describes the proliferation of the BMU cells.

Several factors may disrupt the cross-talk between osteoclasts and osteoblasts thereby causing bone diseases such as osteoporosis or osteopetrosis. In particular, the presence of metastatic cancer cells at the bone microenvironment is one of these factors (Florencio-Silva et al. 2015). Metastasis occurs when cancer cells spread from an initial body part, -like breast or prostate cancer-, to distant tissues, -like brain, lungs or bone-. The 'Seed & Soil' theory (Paget 1889) explains that cancer cells (*the seeds*) have preference to certain microenvironments (*the soil*) to metastasize. Breast and prostate cancers are the most common cancers that have high potential to form bone metastases; the former is known to cause osteolytic lesions, while the latter usually exhibits osteoblastic lesions. There is multiple evidence that supports the idea that there are many complex biochemical interactions between metastatic cells and the bone microenvironment, bringing up the hypothesis of the development of a *vicious cycle* that the BMU cells support cancer cells proliferation (Mundy 2002; Theriault and Theriault 2012).

Considering that one of the main causes of death in cancer patients is metastases formation (Massagué and Obenauf 2016), this disease has received much attention in the last years so to understand its mechanisms. It is known the difficulty and limitations of in vivo and in vitro bone metastasis experiments (Kwakwa et al. 2017), thus mathematical modeling may be another approach to obtain insights about the disease and try to validate some posed biological hypotheses. The number of this kind of works is considerably reduced. Lemaire extensions that model these phenomena include: Wang et al. (2011) in which multiple myeloma-induced bone disease is studied based on the bone remodeling model presented in Pivonka et al. (2008), and Farhat et al. (2017) which focuses specifically to model bone metastatic prostate cancer. Komarova type models that consider BMU-disregulation due to cancer are: Ayati et al. (2010) which focus on multiple myeloma and the BMU dynamics; Garzón-Alvaradob (2012) where both metastatic bone lesions are studied via a switch term included in the model; in Ryser et al. (2012) the OPG concentration is proposed as a key parameter mediating the bone metastasis; Coelho et al. (2016) include parathyroid hormone concentration effects and a novel way to determine the number of active osteoclasts and osteoblasts; and Jerez and Camacho (2018) where a logistic cancer equation is coupled to a Komarova bone remodeling model for describing the bone metastasis vicious cycle. From a new approach, in Dingli et al. (2009) and Warman et al. (2018) treatments for multiple myeloma and prostate cancer-induced bone disease are modeled as evolutionary games.

Despite important advances on understanding bone metastasis mechanisms, this disease is still considered incurable (Juárez et al. 2017). Palliative treatments for bone metastases are used to reduce pain and to prevent adverse consequences such as bone fractures and spinal cord compression. In this work we focus on two bone metastasis palliative treatments: denosumab and radiotherapy. Denosumab is a fully human monoclonal antibody to RANKL that acts similarly as OPG and its effectiveness in delaying the appearance of skeletal related events has been proved (Theriault and Theriault 2012). Some of the side-effects of denosumab are urinary tract infection, upper respiratory infection, hypocalcemia and osteonecrosis of the jaw (Lipton et al. 2016). On the other hand, radiotherapy is a treatment that consists in using radiation beams in localized areas of the body to kill cancer cells by damaging their DNA (Lutz et al. 2017). It is estimated that around 50% of cancer patients receive this treatment (Barker et al. 2015). Bone loss is one of the side-effects related to radiotherapy (Zhang et al. 2018). The search of optimal schedules and doses for these bone metastasis treatments continues (Chow et al. 2016; Lipton et al. 2016; Ganesh et al. 2017).

As we mentioned before, it is difficult to make in vivo or in vitro experiments to study the precise effects of bone metastasis treatments, so mathematical modeling can be an alternative approach. A way to model treatments for some disease is via an optimal control problem associated to the differential model that describes the disease. This framework is based on the idea of minimizing an expression that involves the cost of using a treatment while reducing the hazardous effects by the presence of the disease over time (Lenhart and Workman 2007). This mathematical tool was used by Lemos et al. (2016) to model treatments for multiple myeloma but has also been employed to study treatments in other biomedical models (Swan 1990; Fister et al. 1998; De Pillis and Radunskaya 2003). Here, we are interested to find optimal treatments for

the denosumab and radiation therapies since significant information about effects on BMU and collateral damage is known for both treatments. The latter is essential for the mathematical modeling process and the model validation. It is important to remark that there are other novel treatments with intrinsic relevance, unfortunately we do not have enough information about them. It is our hope that this work can be used to motivate the generalization of our results for different therapies.

In the present work, we propose two optimal control models: one for denosumab treatment, and another for radiotherapy. Both of them are based on the bone metastasis Komarova type model proposed in Jerez and Camacho (2018), that describes the dynamics between cancer cells and the main BMU cells. We consider this model as a starting point since it is possible to obtain explicitly the steady-states associated with the cancer-free and cancer-invasion scenarios. Furthermore, we have conditions for the local stability of these equilibria. We also prove existence and uniqueness of solutions for both optimal control models mentioned previously. Such mathematical achievement is of paramount importance for the numerical analysis of the models. The simulations that we obtain agree qualitatively with clinical observations about the evolution of metastatic tumors on *in silico* experiments and on animal models. Moreover, we explore cancer-BMU dynamics for each treatment under different cancer-invasion scenarios.

The paper is organized as follows. In Sect. 2, the bone metastasis basis model is presented and discussed. Next, in Sect. 3 we propose mathematical models for two bone metastasis treatments (denosumab and radiotherapy) as optimal control problems. In Sects. 4 and 5, an optimal control framework is utilized to show existence and uniqueness of solutions, and also to pose the corresponding optimality systems. Finally, in Sect. 6 qualitative effects of treatment regimes are obtained computationally. Numerical simulations and discussions are presented.

2 Bone metastasis basis model

The model that we consider as a basis is from a previous work (Jerez and Camacho 2018). The main biological assumptions are the following:

- There are autocrine and paracrine communications between osteoclasts (hereafter OCs) and osteoblasts (hereafter OBs) which modifies the recruitment and inhibition rates of the cells (Florencio-Silva et al. 2015). This cross-talk is approximated as a power-law (Komarova et al. 2003).
- Bone metastatic cells (hereafter CCs) express a number of factors such as parathyroid hormone related peptide (PTHrP) and interleukins (ILs) that modify bone homeostasis (Mundy 2002; Ottewell 2016). PTHrP enhances OBs expression of RANKL, thereby increasing the number of active OCs; also, OCs resorb bone which causes the release of growth factors such as TGF-β than increase the production of PTHrP (Mundy 2002). Thus, we assume that the communication between OCs and CCs have positive effects on both populations (mutualism).
- The OBs–CCs communication loop is not completely known (Ottewell 2016). In the case of an osteolytic lesion the presence of OBs may not directly impact the

proliferation of CCs, and vice versa. On the other hand, for an osteoblastic lesion the OBs population may increase due to osteoblast-promoting factors produced by CCs such as IL-6. Therefore, we assume that the communication between OBs and CCs may have positive, negative or null effects on these populations.

- Finally, we also assume that CCs population satisfies a logistic equation which is penalized by a linear elimination rate that reflects the adaptability of CCs to the bone microenvironment (Farhat et al. 2017).

For a schematic representation of the assumptions see Fig. 1.

Let us denote by $C(t)$, $B(t)$ and $T(t)$ the population of OCs, OBs and CCs at a certain time t, respectively. Thus, the basis model is as follows:

$$\frac{dC(t)}{dt} = \underbrace{\alpha_1 C(t)B(t)^{g_1}}_{\text{OCs inhibition by OBs}} - \beta_1 C(t) + \underbrace{\sigma_1 C(t)T(t)}_{\text{OCs promotion by CCs}}, \tag{1a}$$

$$\frac{dB(t)}{dt} = \underbrace{\alpha_2 C(t)^{g_2} B(t)}_{\text{OBs promotion by OCs}} - \beta_2 B(t) + \underbrace{\sigma_2 B(t)T(t)}_{\text{CCs net effect on OBs}}, \tag{1b}$$

$$\frac{dT(t)}{dt} = \alpha_3 T(t)\left(1 - \frac{T(t)}{m}\right) - \beta_3 T(t) + \underbrace{\sigma_3 C(t)^{g_2} T(t)}_{\text{CCs promotion by OCs}} + \underbrace{\sigma_4 B(t)^{g_1} T(t)}_{\text{OBs net effect on CCs}}, \tag{1c}$$

where α_i are the rates of cell production for $i = 1, 2, 3$; β_i are the rates of cell removal; and g_1 and g_2 are the net effectiveness of paracrine factors, see Komarova et al. (2003). The exponent parameters g's codify the effects of complex biochemical reactions on the population dynamics. We assume that $g_1 < 0$ and $g_2 > 0$ which correspond, respectively, to an inhibition from OBs to OCs and to a promotion of OBs due to OCs (Komarova et al. 2003; Jerez and Camacho 2018). The coefficient m is the carrying capacity of the logistic growth rate of CCs within the BMU location. The parameters σ's are the proportional rates of the OCs–CCs and OBs–CCs interactions where we incorporate the possible outcomes of the vicious cycle. Depending on the signs and values of these parameters, the model exhibits osteolytic, osteoblastic or mixed lesion. It is important to remark that some of the proposed models in the literature focus only on one particular primary tumor tissue whereas we aim towards a unified model for describing and understanding more about the intertwined mechanisms of bone metastasis.

2.1 Cancer-free and cancer-invasion equilibria

In Jerez and Camacho (2018), the existence of cancer-free and cancer-invasion steady-states of the model (1) is assured and explicit expressions for them are found. The cancer-free equilibrium is given by

$$\left(\left(\frac{\beta_2}{\alpha_2}\right)^{\frac{1}{g_2}}, \left(\frac{\beta_1}{\alpha_1}\right)^{\frac{1}{g_1}}, 0\right),$$

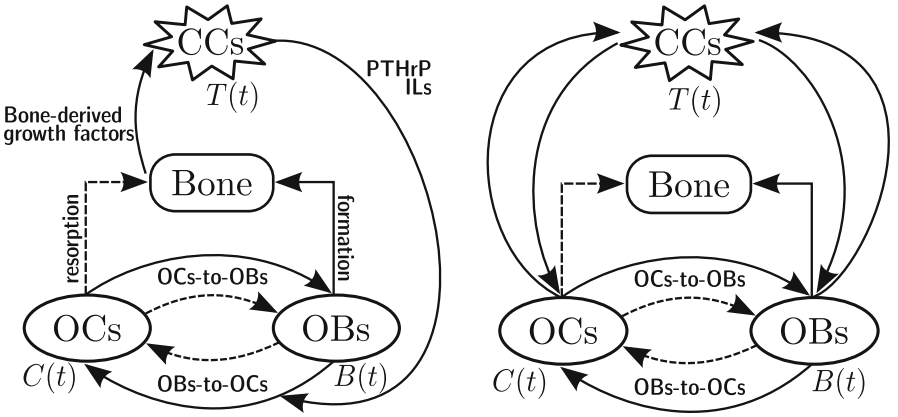

Fig. 1 Diagrams representing simplified interaction networks in an osteolytic lesion (*left*) and in an osteoblastic or mixed lesion (*right*). Dashed lines represent inhibition/degradation (negative) effects, and solid lines represent promotion/formation (positive) effects

which is locally stable if $g_1 g_2 < 0$ and $\frac{\beta_2\sigma_3}{\alpha_2} + \frac{\beta_1\sigma_4}{\alpha_1} < \beta_3 - \alpha_3$. On the other hand, the cancer-invasion equilibrium, denoted by $E_I = (C_I, B_I, T_I)$, can be expressed as:

$$\begin{aligned} C_I &= \left(\frac{\alpha_1(r\beta_2 + \beta_3\sigma_2 - \alpha_3\sigma_2) - \sigma_4(\beta_1\sigma_2 - \beta_2\sigma_1)}{\alpha_1\alpha_2 r + \alpha_1\sigma_2\sigma_3 + \alpha_2\sigma_1\sigma_4} \right)^{\frac{1}{g_2}}, \\ B_I &= \left(\frac{\alpha_2(r\beta_1 + \beta_3\sigma_1 - \alpha_3\sigma_1) - \sigma_3(\beta_1\sigma_2 - \beta_2\sigma_1)}{\alpha_1\alpha_2 r + \alpha_1\sigma_2\sigma_3 + \alpha_2\sigma_1\sigma_4} \right)^{\frac{1}{g_1}}, \\ T_I &= \frac{\alpha_1\alpha_2\alpha_3 - \alpha_1\alpha_2\beta_3 + \alpha_1\sigma_3\beta_2 + \alpha_2\sigma_4\beta_1}{\alpha_1\alpha_2 r + \alpha_1\sigma_2\sigma_3 + \alpha_2\sigma_1\sigma_4}, \end{aligned} \tag{2}$$

where $r = \alpha_3/m$. If $\sigma_2 < 0$ and $\sigma_4 = 0$, then the cancer-invasion steady-state E_I is locally stable if these three inequalities hold:

$$\frac{\beta_3 - \alpha_3}{\sigma_3} < \frac{\beta_2}{\alpha_2}, \quad \frac{|\sigma_2|}{\alpha_2} < \frac{\alpha_3}{\sigma_3}, \quad \text{and} \quad C_I\left(1 - \frac{\alpha_3}{|\sigma_2| g_1}\right) < \frac{\beta_1}{\sigma_1}. \tag{3}$$

Note that if we let $\sigma_2 > 0$ and $\sigma_4 = 0$ then E_I is unstable.

We predict the local behavior of the solutions around the corresponding steady-states being the cancer-invasion equilibrium of great importance. If the cancer-invasion equilibrium is locally stable, then CCs may colonize the bone tissue if there are enough of these cells; if this equilibrium is unstable, then an erratic invasion (increasing oscillations) or an elimination of CCs may occur. This information is be used on Sect. 6 for the numerical simulations results.

3 Bone metastasis treatment models

In this section, we present two mathematical models for bone metastasis treatments: denosumab and radiotherapy treatments. These two treatments modify the cellular behavior of OCs, OBs and CCs. Since these three cellular populations are intertwined in an intricate communication network mediated mainly by biochemical factors, it is difficult to predict the overall dynamics of the BMU under treatments. Our goal is to understand the CCs-BMU dynamics and to address the question about the best way to dose those two treatments. For that matter, we use the optimal control framework where a cost function that includes an input (the treatment) and also undesirable variables (bone metastases) is minimized (Lenhart and Workman 2007). Such optimal control cost includes abstractly an economical cost and the side-effects of the treatment.

3.1 Denosumab treatment model

Denosumab affects the main bone remodeling signaling pathway RANK/RANKL/OPG (Florencio-Silva et al. 2015). The main biological mechanisms that we consider and their corresponding mathematical assumptions are:

- When OBs produce RANKL and this molecule binds to RANK then OCs are activated. Denosumab neutralizes RANKL and it is used to treat bone metastasis to slow down excessive bone resorption caused by the vicious cycle CCs $\rightarrow$ OBs $\rightarrow$ OCs (Mundy 2002; Lipton et al. 2016). For the model, we propose that denosumab alters the cell activity of OCs in a proportional way.
- Denosumab has various side-effects on the patient, such as osteonecrosis of the jaw (Theriault and Theriault 2012). We propose to combine these side-effects and the economical cost of this treatment in a function that measures both components.

Let us denote by $u_D(t)$ the effect of denosumab on the activity of OCs. Considering the previous assumptions, we propose the following denosumab model:

$$\min_{u_D} J(u_D(t)) \quad \text{where} \quad J(u_D(t)) = \int_0^{t_f} \Big(\underbrace{w_D u_D(t)^2}_{\text{DT cost and side-effects}} + T(t)^2 \Big)\, dt \tag{4a}$$

subject to:

$$\frac{dC(t)}{dt} = \alpha_1 \underbrace{(1-u_D(t))}_{\text{DT effects on OCs}} C(t)B(t)^{g_1} - \beta_1 C(t) + \sigma_1 C(t)T(t), \tag{4b}$$

$$\frac{dB(t)}{dt} = \alpha_2 C(t)^{g_2} B(t) - \beta_2 B(t) + \sigma_2 B(t)T(t), \tag{4c}$$

$$\frac{dT(t)}{dt} = \alpha_3 T(t)\left(1 - \frac{T(t)}{m}\right) - \beta_3 T(t) + \sigma_3 C(t)^{g_2} T(t) + \sigma_4 B(t)^{g_1} T(t), \tag{4d}$$

$$C(0),\ B(0),\ T(0) > 0 \quad \text{given}, \tag{4e}$$

$$0 \le u_D(t) \le u_D^{\max} < 1 \quad \text{for all} \quad 0 \le t \le t_f, \tag{4f}$$

where DT stands for denosumab therapy, $u_D \equiv 0$ means that no denosumab is applied and $u_D \equiv u_D^{\max}$ reflects the maximum effectivity of denosumab in nullifying the activity of OCs. The cost functional $J(u_D(t))$ measures the economical cost and side-effects of using denosumab and stores the net side-effects due to the presence of CCs. To construct the cost functional, we follow the standard notion of non-linear cost functionals (Lenhart and Workman 2007). In particular, the cost per unit of time of the presence of CCs is measured by $T(t)^2$, while the use of denosumab produce a cost per unit of time in term of its effectivity $u_D(t)^2$. In the cost functional (4a), the parameter w_D is a weight control parameter that represents the normalized cost of using denosumab. We assume a fixed time window from a starting day 0 to a final day denoted by t_f.

3.2 Radiotherapy treatment model

Another treatment option for patients with bone metastasis is radiotherapy. In Zhang et al. (2018) the authors offers a landscape of what is known about the effects of radiation on the bone cells, particularly on OCs and OBs. We now mention the key biological aspects of radiotherapy and the associated mathematical assumptions:

- The main action of radiotherapy is to disrupt CCs proliferation by damaging their DNA; however, it also affects non-cancerous cells of the body like OCs and OBs (Vakaet and Boterberg 2004; Brenner 2008; Zhang et al. 2018). Therefore, we propose that radiation increases the elimination rates of OCs, OBs and CCs.
- Radiation may cause haematological toxicity, nausea and vomiting (Chow et al. 2016). Taking into account this fact, we include the use of radiation with a function that measures these effects along with the economical cost of the treatment.
- It has been observed that irradiation may impairs bone remodeling in the long run (Oest et al. 2015; Zhang et al. 2018). We propose that the effects of a radiation dose decay exponentially rather than instantly on the BMU.

Let us denote by $u_R(t)$ the cell-killing rate due to radiation on the BMU. Considering the mentioned assumptions, we propose the following radiotherapy model:

$$\min_{u_R} J(u_R(t)) \quad \text{where} \quad J(u_R(t)) = \int_0^{t_f} \Big(\underbrace{w_R u_R(t)^2}_{\text{RT cost and side-effects}} + T(t)^2 \Big)\, dt, \tag{5a}$$

subject to:

$$\frac{dC(t)}{dt} = \alpha_1 C(t) B(t)^{g_1} - \underbrace{(\beta_1 + \psi_1 u_R(t))}_{\text{RT effects on OCs}} C(t) + \sigma_1 C(t) T(t), \tag{5b}$$

$$\frac{dB(t)}{dt} = \alpha_2 C(t)^{g_2} B(t) - \underbrace{(\beta_2 + \psi_2 u_R(t))}_{\text{RT effects on OBs}} B(t) + \sigma_2 B(t) T(t), \tag{5c}$$

$$\frac{dT(t)}{dt} = \alpha_3 T(t) \left(1 - \frac{T(t)}{m}\right) - \underbrace{(\beta_3 + u_R(t))}_{\text{RT effects on CCs}} T(t) + \sigma_3 C(t)^{g_2} T(t) + \sigma_4 B(t)^{g_1} T(t), \tag{5d}$$

$$C(0),\ B(0),\ T(0) > 0 \quad \text{given}, \tag{5e}$$

$$0 \le u_R(t) \le u_R^{\max} \quad \text{for all} \quad 0 \le t \le t_f. \tag{5f}$$

where RT stands for radiotherapy, the parameters $u_R^{\max}$ and w_R are the analogues of $u_D^{\max}$ and w_D as in the denosumab case. Here, we propose to increase linearly the CCs elimination rate β_3 by $u_R(t)$. To account for adverse effects on the proliferation of OCs and OBs, we assume that their respective elimination rates are also affected by radiation as well. For that reason, we introduce the coefficients ψ_1 and ψ_2 that act as rescaling parameters of the radiation effect $u_R(t)$ on OCs and OBs, respectively.

4 Optimal solution for the denosumab model

In order to explore these bone metastasis treatment models, it is important to guarantee the existence of optimal solutions, $u_D(t)$ and $u_R(t)$, that satisfy the corresponding problems (4) and (5). In this section, we prove the existence and also the uniqueness of an optimal control solution to the denosumab treatment model (4), and we discuss how the radiotherapy model (5) has analogous results.

4.1 Existence of optimal solutions

We are interested in studying the effects of bone metastasis treatments on the BMU when the tumor has the potential to establish or has already established a successful invasion. To accomplish this, we assume two possible scenarios related to the boundness and positivity of the solutions for the non-treatment model (1):

Assumption A The cancer-invasion equilibrium is locally stable and the initial conditions are located nearby.

Assumption B The cancer-invasion equilibrium is locally unstable, then we assume *a priori* that the state variables remain inside a compact subset.

Assumption A is valid if the steady-state (2) satisfies conditions (3). Assumption B is a reasonable assumption that has been proposed in other optimal control problems, see for instance (Bara et al. 2017). In either case, these assumptions lead us to consider a compact subset near the cancer-invasion equilibrium from which the solutions stay in that subset for every positive time $t > 0$.

Now, let Ω be a compact subset of the natural domain of model (1) defined by $\Omega^+ = \{(C(t), B(t), T(t)) \mid x_i > 0,\ i = 1, 2, 3\}$. In this subset, the state variables $(C(t), B(t), T(t))$ are uniformly bounded because Ω is a compact subset of Ω^+. This means that, for all $t \in [0, t_f]$, we have

$$C(t) \le C^{\max} \quad \text{and} \quad B(t) \ge B^{\min}.$$

Let us denote the state variables as $x(t) = (C(t), B(t), T(t))$. To prove the existence of an optimal control we employ Theorem 4.1 from Fleming and Rishel (1975). Such

result states that the the following conditions are sufficient to guarantee the existence of an optimal control solution for (4):

- $(H1)$ The right-hand side of the model (4b)–(4d) is composed of continuous functions, and for each one of these functions f_i there exist positive constants C_1, C_2 such that $|f_i(t,x,u_D)| \leq C_1(1+|x|+|u_D|)$ and $|f_i(t,\bar{x},u_D)-f_i(t,x,u_D)| \leq C_2|\bar{x}-x|(1+|u_D|)$ for all $0 \leq t \leq T$ and $i = 1,2,3$.
- $(H2)$ There exists at least one pair $(x(t), u_D(t))$ satisfying both (4b)–(4d) and (4f).
- $(H3)$ The set of admissible controls is closed and convex.
- $(H4)$ The right-hand side of the model is bounded above by a sum of the states and the control, and it can be written as a linear function with respect the control.
- $(H5)$ The integrand of cost functional is convex with respect the control and it is bounded above by $C_3|u_D|^n - C_4$ for some fixed $C_3 > 0$, $C_4 \in \mathbb{R}$ and $n > 1$.

We proceed to show such conditions.

Lemma 1 *The model (4) satisfies $(H1)$.*

Proof It is straightforward since the model functions are of class C^2 in Ω. □

Lemma 2 *There exists at least one pair $(x(t), u_D(t))$ with $u_D \in \mathcal{U}$ such that Eq. (4b)–(4d) is satisfied.*

Proof The condition $(H2)$ is satisfied by the Carathéodory's existence theorem (see Theorem 9.2.1 from Lukes 1982), which guarantees the existence of solutions for Cauchy problems. □

Lemma 3 *The set of admissible controls is closed and convex.*

Proof Since $0 \leq u_D(t) \leq u_D^{\max}$ then the lemma requirements are satisfied. □

Lemma 4 *The right-hand side of (4b)–(4d) is continuous, also it is bounded from above by a sum of the states and the control, and it can be written as a linear function of the control.*

Proof Let $f(t,x,u_D)$ be the vector function defined by the right-hand side of (4b)–(4d). As mentioned above, f is continuous on Ω. Now we have to find suitable bounds for the states. Since $0 < C(t) \leq C^{\max}$, $B^{\min} \leq B(t)$ and $0 < T(t) \leq C^{\max}$, where the constants $C^{\max}$, $B^{\min}$ and $C^{\max}$ come from the definition of the domain Ω, then:

$$\begin{aligned}
\frac{dC(t)}{dt} &= \alpha_1 C(t) B(t)^{g_1}(1-u_D) - \beta_1 C(t) + \sigma_1 C(t) T(t) \\
&\leq \alpha_1 C(t) B(t)^{g_1} - \beta_1 C(t) + \sigma_1 C(t) T(t) \\
&\leq \alpha_1 C(t) m_1 - \beta_1 C(t) + \sigma_1 C(t) T(t) \quad (g_1 < 0 \text{ and } m_1 := (B^{\min})^{g_1}) \\
&\leq \alpha_1 C(t) m_1 + \sigma_1 C(t) T(t) \\
&= C(t)(\alpha_1 m_1 + \sigma_1 C^{\max}), \qquad (6)
\end{aligned}$$

so $dC(t)/dt$ is bounded from above by the linear Eq. (6). Similarly,

$$\frac{dB(t)}{dt} \leq B(t)(\alpha_2 m_2 + \sigma_2 C^{\max}),$$

where $m_2 := (C^{\max})^{g_2}$. Taking into account that: $\sigma_2 \geq 0$ or $\sigma_2 < 0$, then

$$\frac{dB(t)}{dt} \leq \begin{cases} B(t)(\alpha_2 m_2 + \sigma_2 C^{\max}) & \text{if } \sigma_2 \geq 0 \\ B(t)\alpha_2 m_2 & \text{if } \sigma_2 < 0. \end{cases} \tag{7}$$

Hence, $B(t)$ is also bounded from above by a linear equation. Analogous to $C(t)$ and $B(t)$ and considering that $\sigma_4 \leq 0$, we have

$$\frac{dT(t)}{dt} \leq T(t)\left(\alpha_3 - \beta_3 + \sigma_3 m_2\right). \tag{8}$$

From inequalities (6)–(8), we know that the model is bounded from above by a linear system. Thus, the solutions are bounded for a finite final time. Observe that there are two cases given by the sign of σ_2. These inequalities, together with the triangle inequality, also give:

$$\begin{aligned} &|f(t,x,u_D)| \\ &= \left| \left(\frac{dC}{dt}, \frac{dB}{dt}, \frac{dT}{dt} \right)^{\mathsf{T}} \right| \\ &= \left| \begin{pmatrix} \alpha_1 m_1 + \sigma_1 C^{\max} & 0 & 0 \\ 0 & \alpha_2 m_2 + \sigma_2 C^{\max} & 0 \\ 0 & 0 & \alpha_3 - \beta_3 + \sigma_3 m_2 \end{pmatrix} \begin{pmatrix} C \\ B \\ T \end{pmatrix} \right| + \left| \begin{pmatrix} \alpha_1 C^{\max} m_2 \\ 0 \\ 0 \end{pmatrix} u_D \right| \\ &\leq C_1(|x| + |u_D|), \end{aligned} \tag{9}$$

where C_1 depends on the model parameters and the bounds of its solutions. The case for $\sigma_2 < 0$ is analogous. □

Lemma 5 *The integrand from (4a) is convex in the control, and it is bounded from above by $C_3|u_D|^n - C_4$ with $C_3 > 0$ and $n > 1$.*

Proof The integrand $L(t,x,u_D) = T(t)^2 + w_D u_D^2$ is convex respect u_D, and also

$$L(t,x,u_D) = T(t)^2 + w_D u_D^2 \geq w_D u_D^2 = C_3|u_D|^n, \tag{10}$$

with $C_3 = w_D > 0$ and $n = 2 > 1$. □

The above discussion allows us to state the following result:

Theorem 1 *The denosumab treatment model (4), considering the domain Ω, has an optimal control u_D^*.* □

4.2 Optimality system

Under Assumptions A or B we have prove the existence of at least one optimal control. Here, we use Pontryagin's Maximum Principle (Pontryagin et al. 1962; Lenhart and

Workman 2007) to derive necessary conditions that every optimal control satisfies. Let H be the Hamiltonian defined by

$$\begin{aligned} H = &\left(\alpha_1 C(t) B(t)^{g_1} (1 - u_D(t)) - \beta_1 C(t) + \sigma_1 C(t) T(t)\right) \lambda_1(t) \\ &+ \left(\alpha_2 C(t)^{g_2} B(t) - \beta_2 B(t) + \sigma_2 B(t) T(t)\right) \lambda_2(t) \\ &+ \left(\alpha_3 T(t) \left(1 - \frac{T(t)}{m}\right) - \beta_3 T(t) + \sigma_3 C(t)^{g_2} T(t)\right) \lambda_3(t) \\ &+ T(t)^2 + w_D u_D(t)^2. \end{aligned} \tag{11}$$

From (11) we get the following adjoint system for denosumab model (4):

$$\frac{d\lambda_1}{dt} = -\lambda_1 \left(\alpha_1 B^{g_1} (1 - u_D) - \beta_1 + \sigma_1 T\right) - \lambda_2 \left(\alpha_2 g_2 C^{g_2 - 1} B\right) - \lambda_3 \left(\sigma_3 g_2 C^{g_2 - 1} T\right), \tag{12a}$$

$$\frac{d\lambda_2}{dt} = -\lambda_1 \left(\alpha_1 g_1 C B^{g_1 - 1} (1 - u_D)\right) - \lambda_2 \left(\alpha_2 C^{g_2} - \beta_2 + \sigma_2 T\right), \tag{12b}$$

$$\frac{d\lambda_3}{dt} = -\lambda_1 \sigma_1 C - \lambda_2 \sigma_2 B - \lambda_3 \left(\alpha_3 \left(1 - \frac{2T}{m}\right) - \beta_3 + \sigma_3 C^{g_2}\right) - 2T, \tag{12c}$$

$$\lambda_1(t_f) = \lambda_2(t_f) = \lambda_3(t_f) = 0. \tag{12d}$$

The optimality condition for (4), obtained also by means of the Pontryagin's Maximum Principle, is the following:

$$u_D^*(t) = \max\left\{0, \min\left\{1, \frac{\alpha_1 C(t) B(t)^{g_1} \lambda_1(t)}{2 w_D}\right\}\right\}, \tag{13}$$

which is the characterization of every optimal solution u_D^* for (4) in terms of the state variables, the adjoint variables and the parameters of the model. A direct use of the Maximum Principle gives us:

Theorem 2 *Let u_D^* be an optimal control for the denosumab model (4) and $x = (C, B, T)$ its associated state-variable. Then there exist functions $\lambda_1(t)$, $\lambda_2(t)$ and $\lambda_3(t)$ that satisfy the adjoint system (12). Also, the optimal control u_D^* satisfies the optimality condition (13).* □

4.3 Uniqueness of optimal solutions

In order to prove the uniqueness of an optimal control problem, we follow the steps proposed in Fister et al. (1998) and state the next theorem:

Theorem 3 *There exists a final time t_f such that the model (4) has a unique optimal control solution.*

Proof See Appendix. □

5 Optimal solution for the radiotherapy model

Besides the denosumab treatment, we also explore the radiotherapy effects on the dynamics of the bone metastasis model. In this section, we give the optimality system and discuss about the existence and uniqueness of the optimal control for the radiotherapy model (5).

5.1 Existence of optimal solutions

The five lemmas for the existence of solutions of the denosumab model are proved in the same way for the radiotherapy treatment model, since they have a similar structure: an *a priori* bounded domain, a bounded control u_R, and the model is linear respect to u_R. Thus, similar algebraic manipulations give the existence of solutions for the radiotherapy model.

5.2 Optimality system

Analogously as in the denosumab model, using the Maximum Principle we obtain the following optimality system for the radiotherapy model (5):

$$\frac{dC}{dt} = \alpha_1 C B^{g_1} - (\beta_1 + \psi_1 u_R^*)C + \sigma_1 CT, \tag{14a}$$

$$\frac{dB}{dt} = \alpha_2 C^{g_2} B - (\beta_2 + \psi_2 u_R^*)B + \sigma_2 BT, \tag{14b}$$

$$\frac{dT}{dt} = \alpha_3 T\left(1 - \frac{T}{m}\right) - (\beta_3 + u_R^*)T + \sigma_3 C^{g_2} T + \sigma_4 B^{g_1} T, \tag{14c}$$

$$\frac{d\lambda_1}{dt} = -\alpha_2 g_2 \lambda_2 C^{g_2 - 1} B - \sigma_3 g_2 \lambda_3 C^{g_2 - 1} T - \left(\alpha_1 B^{g_1} + \sigma_1 T - \beta_1 - \psi_1 u_R^*\right)\lambda_1, \tag{14d}$$

$$\frac{d\lambda_2}{dt} = -\alpha_1 g_1 \lambda_1 C B^{g_1 - 1} - \sigma_4 g_1 \lambda_3 B^{g_1 - 1} T - \left(\alpha_2 C^{g_2} + \sigma_2 T - \beta_2 - \psi_2 u_R^*\right)\lambda_2, \tag{14e}$$

$$\begin{aligned}\frac{d\lambda_3}{dt} = &-\sigma_1 \lambda_1 C - \sigma_2 \lambda_2 B - \left(\sigma_3 C(t)^{g_2} + \sigma_4 B^{g_1} - \alpha_3\left(\frac{T}{m} - 1\right)\right.\\ &\left. -\beta_3 - u_R^* - \frac{\alpha_3 T}{m}\right)\lambda_3 - 2T,\end{aligned}$$

$$C(0), B(0), T(0) \quad \text{given}, \tag{14f}$$

$$\lambda_1(t_f) = \lambda_2(t_f) = \lambda_3(t_f) = 0, \tag{14g}$$

$$u_R^*(t) = \max\left\{0, \min\left\{1, \frac{\psi_1 C(t)\lambda_1(t) + \psi_2 B(t)\lambda_2(t) + T(t)\lambda_3(t)}{2w_R}\right\}\right\}. \tag{14h}$$

5.3 Uniqueness of optimal solutions

Uniqueness of optimal solutions for the radiotherapy model is analogous to the denosumab case since changes in the model (ODEs, cost functional or control restrictions) produce a similar effect in the optimality system (adjoint system and optimality condition).

6 Numerical results and discussion

The existence and uniqueness of solutions guarantee that a convergent numerical method will get the approximation to the unique optimal solution. Taking advantage of that, here we use the forward-backward sweep method (FBSM) (Lenhart and Workman 2007). This numerical scheme is based upon the iterative use of the Maximum Principle. Considering the optimal control problem for the denosumab model (4) together with its adjoint system (12) and the optimality condition (13), the steps involved in the FBSM are the following:

1. Propose an initial control $u_D^0(t)$.
2. Solve forward in time the state variable system (4).
3. Solve backward in time the adjoint system (12).
4. Use the Maximum Principle to get a new control update u_D^k for step k. Here, we consider (Lenhart and Workman 2007):

$$u_D^k(t) \hookleftarrow \mu u_D^k(t) + (1-\mu)u_D^{k-1}(t).$$

   If a convergence criteria is met, e.g., the control update is close to previous control, then STOP; else, return to STEP 2.

For solving the forward and backward ODEs, we used a fourth order Runge–Kutta scheme with variable time step. Let us point out that the problem about the convergence of the FBSM is discussed in McAsey et al. (2012). In that work, the authors prove results about the convergence of the FBSM, and the main hypotheses required to guarantee such convergence are Lipschitz conditions, an appropriate length for the integration interval and boundedness of the adjoint system. Some of these conditions, in particular the last one, are difficult to satisfy *a priori* because of the non-linearities of the treatment models.

To achieve convergence, here we set the maximum value of the control u_D to $u_D^{\max} = 0.6$ instead of using $u_D^{\max} = 1$. From a modeling perspective, this means that we assume that the treatment does not have a complete effectiveness. An example of this approach, used in a different problem, can be found in Stephenson et al. (2017). Also, we initialized the control u^0 for the FBSM as $u^0 \equiv u_D^{\max}$. We have convergence of the simulations when μ takes values within the interval $0.15 \leq \mu \leq 0.6$.

Table 1 Fixed global parameter values, see Sect. 6.1 for discussion

Parameter	Value	Description	Reference
g_1	-0.3	Net paracrine effectiveness on OCs	Jerez and Camacho (2018)
g_2	0.7	Net paracrine effectiveness on OBs	Assumed
α_1	0.5	Activity on OCs production	Assumed
α_2	0.05	Activity on OBs production	Assumed
β_1	0.2	OCs removal rate	Komarova et al. (2003)
β_2	0.02	OBs removal rate	Komarova et al. (2003)
β_3	0	Elimination rate of CCs	Assumed
σ_2	0	Rate of OBs production by cancer	Assumed
m	10^4	CCs carrying capacity	Farhat et al. (2017)
$\psi_1,\ \psi_2$	1	Effect of radiation on OCs and OBs	Assumed

6.1 Parameters for numerical simulations

After exploring numerous combinations for the parameter values, and in an effort to agree with experimental data (Komarova et al. 2003; Farhat et al. 2017; Araujo et al. 2014), we considered a fixed set of values for certain parameters depicted in Table 1 for models (4) and (5). Next, we discuss their selection:

- Initial condition $(C(0), B(0), T(0))$: We chose the initial conditions $C(0) = 4 \times 10^{-6}$, $B(0) = 4$ and $T(0) = 1000$ according with (Komarova et al. 2003; Jerez and Chen 2015).
- The net effectiveness parameters g_1 and g_2: We preserved OBs-induced inhibition on OCs by taking $g_1 = -0.3$ as in Jerez and Chen (2015). However, in this work we increased g_2 from 0.5 (Jerez and Camacho 2018) to 0.7 in order to have a more active remodeling process, that is, larger amplitudes and shorter periods for the OCs and OBs solutions without cancer.
- The cell activity parameters α_1 and α_2: By fixing values of g_1 and g_2 we estimated through trial and error these parameters to obtain standard numbers of OCs and OBs with and without cancer.
- The elimination rates β_1 and β_2: They are proposed as in Komarova et al. (2003).
- Coefficients for CCs: The elimination rate β_3 is considered zero since we include its effect in α_3, having a net production rate for CCs. For the production rate of CCs, α_3, we take a realistic interval based on (Ayati et al. 2010; Farhat et al. 2017). We estimated a normal carrying capacity for the CCs, m, using (Farhat et al. 2017).
- Rates of the OCs-CCs and OBs–CCs interactions σ_i $(i = 1, \ldots, 4)$: They are difficult to estimate *a priori* since we do not have experimental data. So, a trial and error parameter space exploration was made. Election criteria for their values took into consideration the cancer-invasion equilibrium value (2) together with its stability conditions (3), see Fig. 2. Values for these parameters were discarded when erratic numbers of OCs or OBs were presented.
- The radiotherapy control parameters ψ_j $(j = 1, 2)$: They are equal to 1 as a first approach. This selection arises from the observation that other values do not

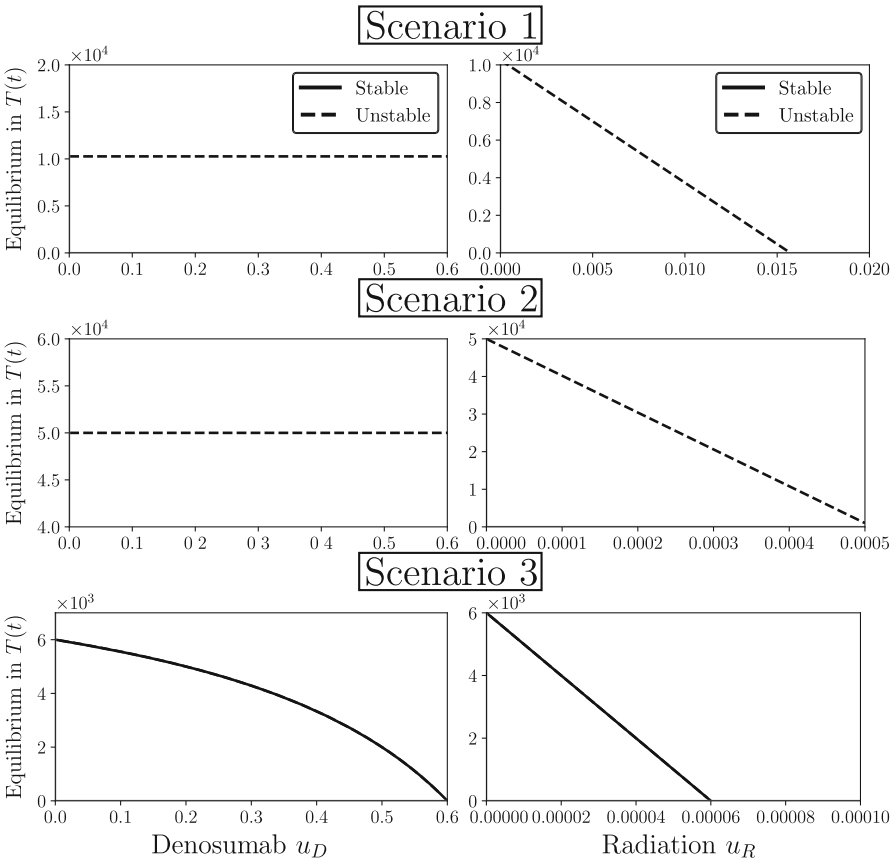

Fig. 2 Bifurcation diagrams corresponding to Scenarios 1–3. The y-axis is the $T(t)$-coordinate of the corresponding cancer-invasion steady-state T_I given in (2)–(3). Left. Denosumab treatment model with bifurcation parameter u_D. Right. Radiotherapy model with bifurcation parameter u_R

change the qualitative behavior of the optimal solutions in our parameter space exploration.

To complement these fixed parameters, we varied the values for α_3, σ_1, σ_3 and σ_4 and obtained three metastatic invasion scenarios; their values are condensed in Table 2. These three scenarios are of biological relevance because they are associated with different dynamics of invasion which may be presented in different physiological settings (Mundy 2002; Ottewell 2016).

6.2 Denosumab treatment

As mentioned before, the function of denosumab is to inhibit osteoclasts activation through RANK-RANKL bindings. Since it is only a palliative treatment, it is expected that only osteoclasts-dependent bone metastatic invasions are heavily affected by means of denosumab administration.

Table 2 Parameters for three different scenarios of the metastatic invasion

Parameter	Scenario 1	Scenario 2	Scenario 3
α_3	1.5×10^{-2}	1×10^{-4}	1×10^{-4}
σ_1	1×10^{-6}	1×10^{-6}	0.0
σ_3	1×10^{-3}	1×10^{-3}	1×10^{-8}
σ_4	0.0	0.0	-1×10^{-4}

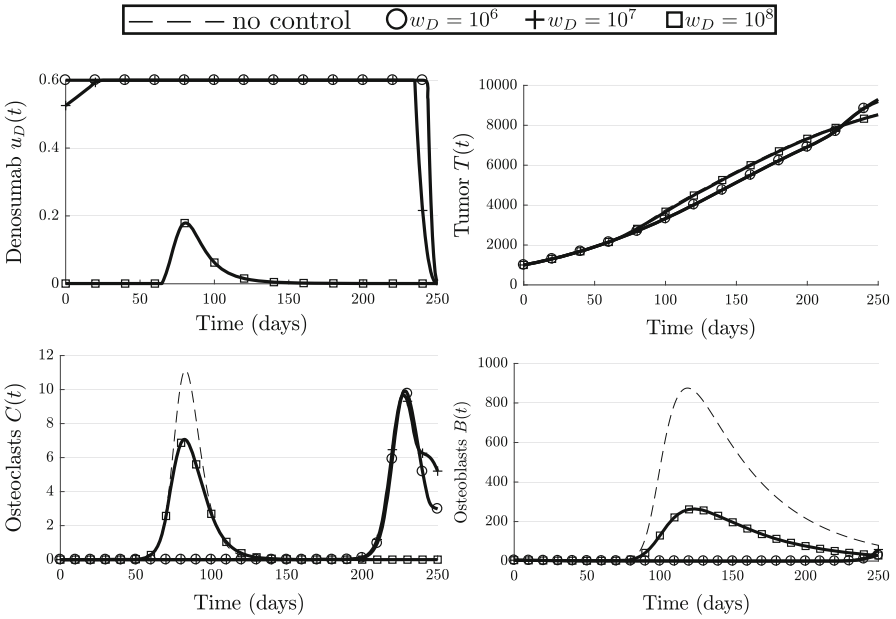

Fig. 3 Scenario 1 for denosumab treatment model for three different cost weight values

Scenario 1: Aggressive metastasis

In this case, the proliferation of CCs is rapid and so this scenario represents an aggressive type of bone metastasis tumor. It may be noted that we are considering in this case that OBs do not affect directly the CCs dynamics ($\sigma_4 = 0$). In Fig. 2, we show that the cancer-invasion steady-state is unstable for all relevant values of α_1 (from 0 to its actual value 0.5). Also, it can be noted that the cancer-coordinate does not change its value in this range. That means that the steady-state is not changed in this coordinate albeit a treatment is applied.

In Fig. 3, it can be noted that the optimal treatment obtained is an aggressive one: the maximum amount of effectivity ($u_{\max}$) is maintained during almost all the time range, and then is suspended abruptly. Also, we observe that OCs wave is displaced in time but maintains its normal amplitude. Due to the cross-regulation between bone cell populations, this will cause also a displacement of the OBs wave (not seen in the selected time range). However, CCs are indifferent to the decrease of OCs and OBs.

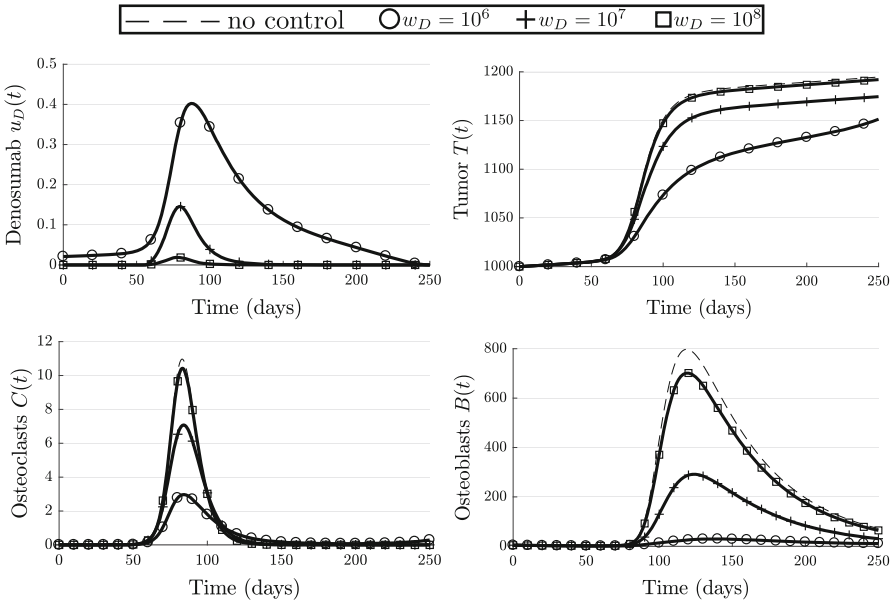

Fig. 4 Scenario 2 for denosumab treatment model

We assume that the proliferation α_3 is high enough to pull the dynamics of CCs away from the bone resorption contribution σ_1. Thus, this scenario presents a metastatic tumor that does not rely completely on the BMU dynamics. As such, the treatment shows to be ineffective, which is clinically observed on advanced aggressive bone metastatic patients (Coelho et al. 2016).

Scenario 2: Osteoclasts-dependent metastasis

In this case the metastatic tumor has a noticeable change when the OCs waves are reduced. In Fig. 2 there is a similar bifurcation diagram as in scenario 1: stability and value of the cancer coordinate do not change with variations of the α_1 parameter.

It can be noted in Fig. 4, that the optimal solution obtained has a maximum amplitude (having a value around 0.4) almost the half of the value of $u_{\max}$; also, its shape is similar to the one of the OCs wave. The treatment applied causes the OCs wave to diminish in amplitude but preserves its appearance in time. The effect of this is also a smaller amplitude on the OBs wave. By contrast from the first case, the CCs population has a visible effect (reduction of 5% compared with the non-treatment case). This is a metastatic invasion that depends more on the BMU dynamics than the previous scenario. The parameters election for this scenario suggests that the tumor depends on the OCs dynamics rather than on the OBs evolution ($\sigma_3 > 0$ and $\sigma_4 = 0$). In this case, treatment regimes show to be more effective than the previous scenario; this is due to the OCs-activity dependence of the CCs proliferation.

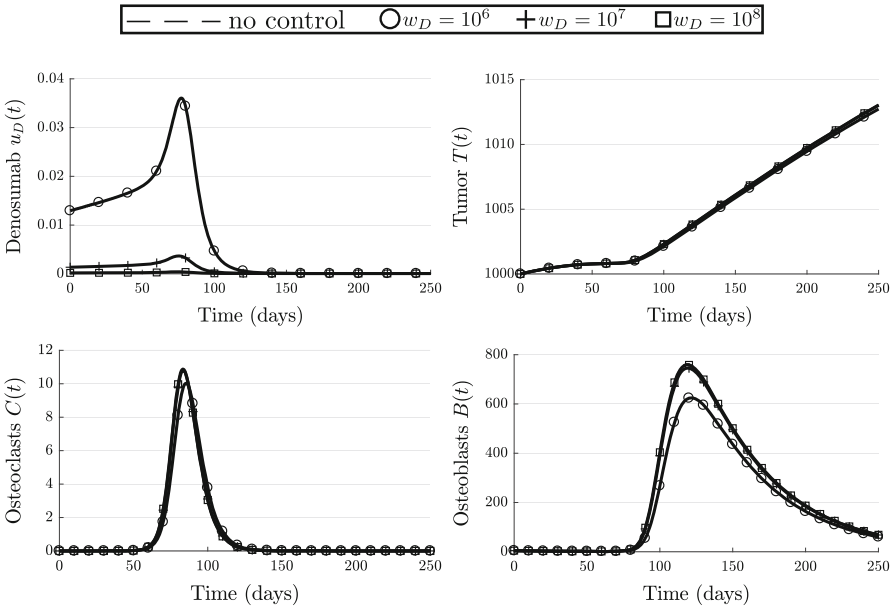

Fig. 5 Scenario 3 for denosumab treatment model

Scenario 3: Slow, BMU-dependent metastasis

In Fig. 2 a different bifurcation diagram is present for scenario 3. The steady-state branch now goes to zero when the parameter α_1 decreases, and the stability does not change from $\alpha_1 = 0.5$ to $\alpha_1 = 0.2$. This suggests that a strong inhibition over the OCs activation would lead the CCs population to be eradicated.

In Fig. 5, however, the optimal solution obtained is to apply the treatment almost to the lowest levels. The amplitudes of the OCs and OBs waves decrease by a small amount and the CCs burden maintains nearly to the same quantity. This simulation suggests that increasing the use of the treatment, even if it drops CCs numbers to a lower level, is more expensive than the cost produced for the reduction of the CCs population with stronger doses. In other words, the metastatic tumor grows or reduces slowly. It is predicted that if the value of w_D is lowered then the optimal solution would take into account a stronger inhibition on OCs.

We tested such hypothesis by changing the value of w_D to 1×10^4. The results from the simulation are shown in Fig. 6. The inhibition of OCs activation lasts longer and the metastatic burden decreases more than with the previous values of w_D. Yet, the OCs wave appearance delays considerable due to the inhibition applied by the treatment and so the amplitude of the OCs wave increases considerably (3-fold the usual). Thus, the OBs wave also increases to drastic levels compared to the untreated case. Both abnormal waves have a positive effect on the metastatic tumor at the end of the treatment. Here, we note that it may be interesting to study how the secondary effects of a treatment may impact the appearance and the amplitude of the OCs and OBs waves.

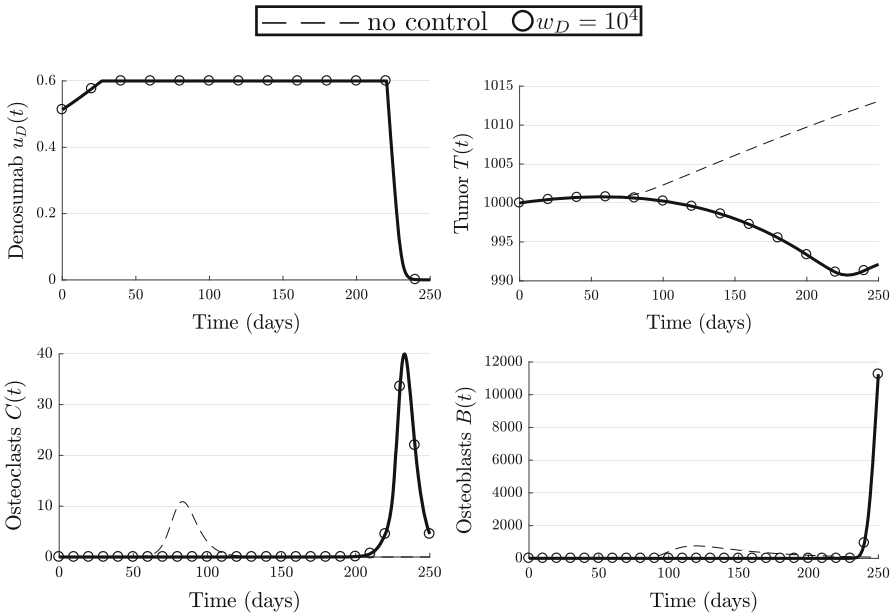

Fig. 6 Scenario 3 for denosumab treatment. The cost parameter is changed to $w_D = 1 \times 10^4$

6.3 Radiotherapy treatment

We adapted the FBSM to find approximations of optimal solutions also for the radiotherapy model (14a). For this model convergence of the method was less sensitive than the denosumab treatment model. In Figs. 7, 8 and 9 are shown the same three scenarios given by Tables 1 and 2 but using the radiotherapy treatment model (14a).

Scenario 1: Aggressive metastasis

In the first scenario, in Fig. 7), there are two optimal solutions that are aggressive (maximum radiation effectivity present). The effects on the OCs and OBs populations are similar under the three treatment regimes. The CCs population decreases its proliferation rate considerably but maintains a prevalent level. It can be noticed that during the OCs wave activation there is a slight increase in the CCs population.

Scenario 2: Osteoclasts-dependent metastasis

In the second scenario, Fig. 8, only one treatment regimen reaches the maximum value 0.015. The difference on the effects of applying the treatment are more noticeable than in the first scenario. But, as in the previous one, OCs and OBs populations do not change much. It is interesting to observe that under the first two treatments (with $w_R = 1 \times 10^9$ and $w_R = 1 \times 10^{10}$) the CCs population shows a slight increase during

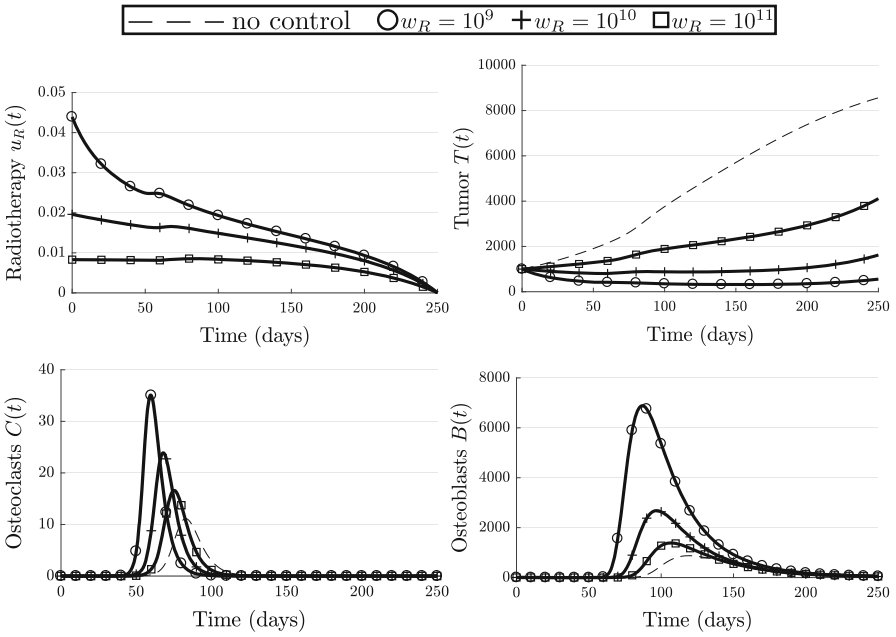

Fig. 7 Scenario 1 for radiotherapy treatment model for three different cost weight values

the remodeling wave activation; in these two regimes the CCs population drops down to lower levels.

Scenario 3: Slow, BMU-dependent metastasis

The third scenario, Fig. 9, is rather similar to the second one. The main difference is that, in this case, the CCs population does not show a significant increase during activation of OCs and OBs waves.

6.4 Summary of numerical simulations

In this section, we explored three scenarios corresponding to different responses of the bone metastatic tumor to the microenvironment: a reckless tumor, a tumor that relies on bone resorption, and a tumor that depends on both bone cell populations.

By bifurcation diagram from Fig. 2, we could predict that, for the particular values of the model parameters, the denosumab treatment is only effective in the third scenario, which is the BMU dependent tumor. And even so, when the weight parameter w_D is large enough then a stronger denosumab treatment is more expensive even if it has the ability to reduce the tumor size. The simulations from Figs. 3, 4, 5 and 6 reflect some possible outputs for the cellular dynamics changes under a denosumab treatment that seeks to minimize economical cost and side-effects.

Similarly, the radiotherapy model was numerically explored in Figs. 7, 8, and 9. In contrast to the denosumab treatment model, the bifurcation diagram reveals that

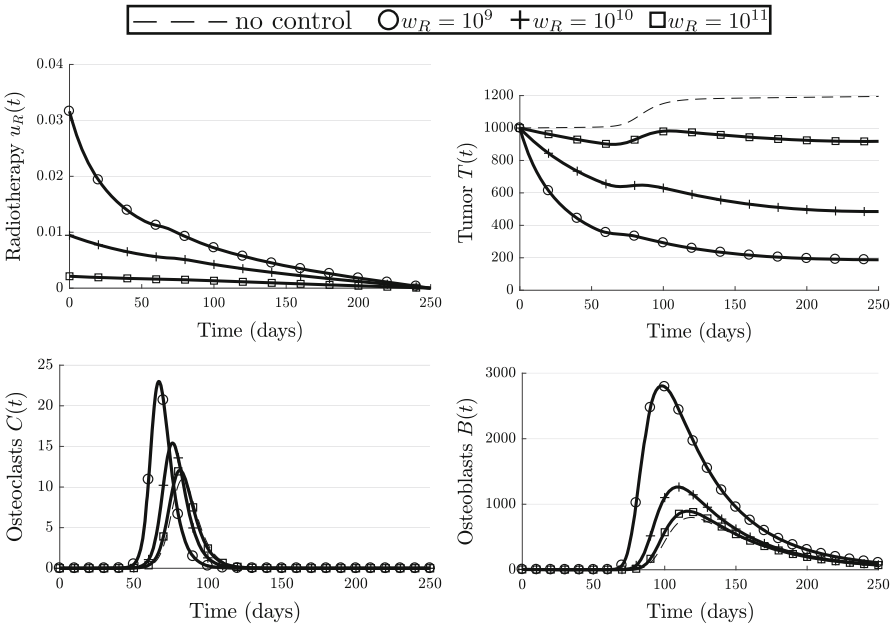

Fig. 8 Scenario 2 for radiotherapy treatment model

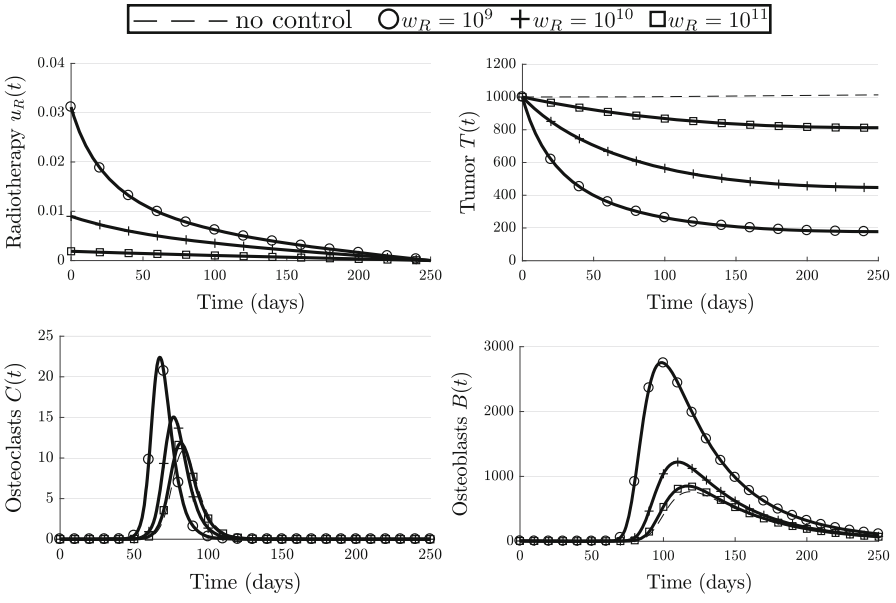

Fig. 9 Scenario 3 for radiotherapy treatment model

radiation has a high potential to bring down the tumor at equilibrium. Another difference in comparison to the denosumab treatment model is that for the radiotherapy model we assumed that radiation also alters the elimination rates of the bone cells. The numerical simulations show interesting cellular dynamics.

Even though that in appearance the radiotherapy shows a better performance in reducing the bone metastasis tumor that the denosumab treatment, it is important to point out that in the numerical simulations radiation has weight parameters that surpass by at least three orders of magnitude the ones assigned for the denosumab treatment. This implies that radiation was assigned a higher cost in terms of economical cost and also from the point of view of the side-effects. Increasing the weight parameters for radiation would translate in affecting less the growth of the tumor.

7 Conclusions

Bone metastasis disease is considered incurable. At the time, several palliative treatments aim towards slowing down the growth of secondary tumors in the bone. These treatments may increase their performance if optimal dosages could be found.

In this work, two bone metastasis treatment models are presented extending a previous model that studies the dynamics of the BMU cells (osteoclasts and osteoblasts) and bone metastatic cancer cells. Having explicit expressions for the steady-states and conditions for their local stability, an exploration of parameters was made in order to find a multitude of dynamics that have already been seen qualitatively in experiments. The objective was to find and analyze treatment regimes for two kind of treatments (denosumab and radiotherapy) and also to study their effects on the cellular dynamics. An optimal control approach incorporates a cost function of the treatment use reflecting the economical cost and also side-effects.

Having knowledge of how the cancer-invasion equilibrium changes locally according to variations of certain parameters is very useful. We presented simulations that allowed us to verify if denosumab and radiation treatments are effective to reduce cancer cell levels. We considered a number of possible relevant scenarios of bone metastatic evolution under treatment. In all of them, the optimal treatment regime obtained depends on the manipulation of the remodeling wave (amplitude or time of appearance). In some cases, the cancer cell populations are already aggressive enough to be influenced by the inhibition of osteoclasts; in other cases, their dependence is rather low and so the metastatic burden is not decreased enough, or it may be decreased at cost of disrupting the osteoclasts-osteoblasts cross-talk in a negative way. Thus, the inhibition of osteoclasts is not always the best answer depending on the type of metastatic cancer residing in the bone microenvironment. As predicted, denosumab treatment poses a weak choice in terms of controlling the growth of the tumor in general. Radiation treatment has a higher potential than the previous one, but the effects on the bone cells still need to be analyzed. Also, radiation has long-run side-effects and important economical cost that limit its applicability. A treatment that respects the natural microenvironment while attacking cancer cells would be more effective and desirable.

We have also observed that the weight parameter of the cost functional does have an important role: if the cost of use of the treatment is rather high then the optimal solution would be to apply low-dose treatments but avoiding a reduction of the metastatic burden.

Thus, it would be interesting to explore alternative treatment strategies by considering other potential control terms. For example, it could be interesting to explore a mathematical model that uses both controls, denosumab and radiation, and evaluate if they can act in a more effective way towards eradicating bone metastasis. Another alternative would be to explore a control that halts interactions between cancer and osteoclasts and osteoblasts by inhibiting other key molecules rather than RANKL, like ILs or PTHrP.

Whereas the optimal control framework is still used in numerous works, it prevails an urgent need to translate real quantitative data (economic cost of treatment, number of skeletal-related events and other side-effects of using the treatment, number of cells in a specific bone metastasis, and others) into the mathematical modeling language to convert these types of models into predictive tools towards the development of patient-personalized treatments. We visualize our results as a step forward to accomplish such goal.

Acknowledgements The authors are grateful to the anonymous reviewers, whose careful observations and helpful suggestions improved considerably the quality of this work. Moreover, AC thanks CONACyT for the Graduate Fellowship Grant 412803. Finally, this work was partially supported by Mexico CONACyT Project CB2016-286437.

Appendix A: Proof of Theorem 2

We follow (Fister et al. 1998) to show uniqueness of the optimal solution for the model (4) under certain conditions over the final time. First, we state some basic results.

Lemma 6 *Let $a, b, c, \bar{a}, \bar{b}, \bar{c}$ be real positive numbers such that they are bounded by some positive constant M. Then*

i) $ab - \bar{a}\bar{b} \leq M(|a - \bar{a}| + |b - \bar{b}|)$.
ii) $(ab - \bar{a}\bar{b})(c - \bar{c}) \leq M((a - \bar{a})^2 + (b - \bar{b})^2 + (c - \bar{c})^2)$.

□

Now, we proceed to prove Theorem 3.

Proof Let suppose that there are two optimal pairs (x, λ, u) and $(\bar{x}, \bar{\lambda}, \bar{u})$ that solve the problem (4) and the adjoint system (12), where $u = u_D$, $x = (x_1, x_2, x_3)$, $x_1 = C$, $x_2 = B$, $x_3 = T$, and $\lambda = (\lambda_1, \lambda_2, \lambda_3)$. Let $m > 0$ be fixed. Then there exist functions y_1, y_2, y_3 and μ_1, μ_2, μ_3 (also with bar) such that $x_i = y_i e^{mt}$, $\bar{x}_i = y_i e^{mt}$, $\lambda_i = \mu_i e^{-mt}$, $\bar{\lambda}_i = \bar{\mu}_i e^{-mt}$. Then:

$$u = \max\left\{0, \min\left\{1, \frac{\alpha_1 e^{mg_1 t} y_1 y_2^{g_1} \mu_1}{2B}\right\}\right\},$$

$$\bar{u} = \max\left\{0, \min\left\{1, \frac{\alpha_1 e^{mg_1 t}\bar{y}_1\bar{y}_2^{g_1}\bar{\mu}_1}{2B}\right\}\right\}.$$

Substituting into the optimality system (4b)–(4d) and (12) we get:

$$\begin{aligned}
y_1'e^{mt} + my_1e^{mt} =&\alpha_1 e^{mt}e^{mg_1 t}y_1y_2^{g_1}(1-u) - \beta_1 e^{mt}y_1 + \sigma_1 e^{2mt}y_1y_3,\\
y_2'e^{mt} + my_2e^{mt} =&\alpha_2 e^{mg_2 t}e^{mt}y_1^{g_2}y_2 - \beta_2 e^{mt}y_2 + \sigma_2 e^{2mt}y_2y_3,\\
y_3'e^{mt} + my_3e^{mt} =&\alpha_3 e^{mt}y_3\left(1 - e^{mt}y_3/K\right) - \beta_3 e^{mt}y_3 + \sigma_3 e^{mg_2 t}e^{mt}y_1^{g_2}y_3\\
&+ \sigma_4 e^{mg_1 t}e^{mt}y_2^{g_1}y_3,\\
\mu_1'e^{-mt} - m\mu_1e^{-mt} =&-e^{-mt}\mu_1(\alpha_1 e^{mg_1 t}y_2^{g_1}(1-u) - \beta_1 + \sigma_1 e^{mt}y_3)\\
&-e^{-mt}\mu_2(\alpha_2 g_2 e^{m(g_2-1)t}y_1^{g_2-1}e^{mt}y_2)\\
&-e^{-mt}\mu_3(\sigma_3 g_2 e^{m(g_2-1)t}y_1^{g_2-1}e^{mt}y_3),\\
\mu_2'e^{-mt} - m\mu_2e^{-mt} =&-e^{-mt}\mu_1(\alpha_1 g_1 e^{mt}e^{m(g_1-1)t}y_1y_2^{g_1-1}(1-u))\\
&-e^{-mt}\mu_2(\alpha_2 e^{mg_2 t}y_1^{g_2} - \beta_2 + \sigma_2 e^{mt}y_3)\\
&-e^{-mt}\mu_3(\sigma_4 g_1 e^{m(g_1-1)t}y_2^{g_1-1}e^{mt}y_3),\\
\mu_3'e^{-mt} - m\mu_3e^{-mt} =&-e^{-mt}\mu_1(\sigma_1 e^{mt}y_1) - e^{-mt}\mu_2(\sigma_2 e^{mt}y_2)\\
&-e^{-mt}\mu_3(\alpha_3(1-2e^{mt}y_3/K) - \beta_3\\
&+\sigma_3 e^{mg_2 t}y_1^{g_2} + \sigma_4 e^{mg_1 t}y_2^{g_1})\\
&-2e^{mt}y_3.
\end{aligned}$$

We can divide the first three equations by e^{mt} and the other three by e^{-mt}. Simplifying:

$$\begin{aligned}
y_1' + my_1 =&\alpha_1 e^{mg_1 t}y_1y_2^{g_1}(1-u) - \beta_1 y_1 + \sigma_1 e^{mt}y_1y_3,\\
y_2' + my_2 =&\alpha_2 e^{mg_2 t}y_1^{g_2}y_2 - \beta_2 y_2 + \sigma_2 e^{mt}y_2y_3,\\
y_3' + my_3 =&\alpha_3 y_3\left(1 - e^{mt}y_3/K\right) - \beta_3 y_3 + \sigma_3 e^{mg_2 t}y_1^{g_2}y_3 + \sigma_4 e^{mg_1 t}y_2^{g_1}y_3,\\
\mu_1' - m\mu_1 =&-\mu_1(\alpha_1 e^{mg_1 t}y_2^{g_1}(1-u) - \beta_1 + \sigma_1 e^{mt}y_3) - \mu_2(\alpha_2 g_2 e^{mg_2 t}y_1^{g_2-1}y_2)\\
&-\mu_3(\sigma_3 g_2 e^{mg_2 t}y_1^{g_2-1}y_3),\\
\mu_2' - m\mu_2 =&-\mu_1(\alpha_1 g_1 e^{mg_1 t}y_1y_2^{g_1-1}(1-u)) - \mu_2(\alpha_2 e^{mg_2 t}y_1^{g_2} - \beta_2 + \sigma_2 e^{mt}y_3)\\
&-\mu_3(\sigma_4 g_1 e^{mg_1 t}y_2^{g_1-1}y_3),\\
\mu_3' - m\mu_3 =&-\mu_1(\sigma_1 e^{mt}y_1) - \mu_2(\sigma_2 e^{mt}y_2)\\
&-\mu_3(\alpha_3(1-2e^{mt}y_3/K) - \beta_3 + \sigma_3 e^{mg_2 t}y_1^{g_2} + \sigma_4 e^{mg_1 t}y_2^{g_1}) - 2e^{2mt}y_3.
\end{aligned}$$

The system related to the other optimal solution $(\bar{x}, \bar{\lambda}, \bar{u})$ is analogous. Subtracting the corresponding equations related to (x, λ, u) and $(\bar{x}, \bar{\lambda}, \bar{u})$ we get:

$$\begin{aligned}
(y_1 - \bar{y_1})' + m(y_1 - \bar{y_1}) =&\alpha_1 e^{mg_1 t}(y_1y_2^{g_1}(1-u) - \bar{y_1}\bar{y_2}^{g_1}(1-\bar{u}))\\
&-\beta_1(y_1 - \bar{y_1}) + \sigma_1 e^{mt}(y_1y_3 - \bar{y_1}\bar{y_3}),
\end{aligned}$$

$$
\begin{aligned}
(y_2-\bar{y_2})'+m(y_2-\bar{y_2}) =& \alpha_2 e^{mg_2t}(y_1^{g_2}y_2-\bar{y_1}^{g_2}\bar{y_2})-\beta_2(y_2-\bar{y_2})\\
&+\sigma_2 e^{mt}(y_2y_3-\bar{y_2}\bar{y_3}),\\
(y_3-\bar{y_3})'+m(y_3-\bar{y_3}) =& \alpha_3\left((y_3-\bar{y_3})-e^{mt}(y_3^2-\bar{y_3}^2)/K\right)\\
&-\beta_3(y_3-\bar{y_3})+\sigma_3 e^{mg_2t}(y_1^{g_2}y_3-\bar{y_1}^{g_2}\bar{y_3})\\
&+\sigma_4 e^{mg_1t}(y_2^{g_1}y_3-\bar{y_2}^{g_1}\bar{y_3}),\\
(\mu_1-\bar{\mu_1})'-m(\mu_1-\bar{\mu_1}) =& -\alpha_1 e^{mg_1t}(\mu_1 y_2^{g_1}-\bar{\mu_1}\bar{y_2}^{g_1})\\
&+\alpha_1 e^{mg_1t}(\mu_1 y_2^{g_1}u-\bar{\mu_1}\bar{y_2}^{g_1}\bar{u})\\
&+\beta_1(\mu_1-\bar{\mu_1})-\sigma_1 e^{mt}(\mu_1y_3-\bar{\mu_1}\bar{y_3})\\
&-\alpha_2 g_2 e^{mg_2t}(\mu_2 y_1^{g_2-1}y_2-\bar{\mu_2}\bar{y_1}^{g_2-1}\bar{y_2})\\
&-\sigma_3 g_2 e^{mg_2t}(\mu_3 y_1^{g_2-1}y_3-\bar{\mu_3}\bar{y_1}^{g_2-1}\bar{y_3}),\\
(\mu_2-\bar{\mu_2})'-m(\mu_2-\bar{\mu_2}) =& -\alpha_1 g_1 e^{mg_1t}(\mu_1y_1y_2^{g_1-1}-\bar{\mu_1}\bar{y_1}\bar{y_2}^{g_1-1})\\
&+\alpha_1 g_1 e^{mg_1t}(\mu_1y_1y_2^{g_1-1}u-\bar{\mu_1}\bar{y_1}\bar{y_2}^{g_1-1}\bar{u})\\
&-\alpha_2 e^{mg_2t}(\mu_2 y_1^{g_2}-\bar{\mu_2}\bar{y_1}^{g_2})\\
&+\beta_2(\mu_2-\bar{\mu_2})-\sigma_2 e^{mt}(\mu_2y_3-\bar{\mu_2}\bar{y_3})\\
&-\sigma_4 g_1 e^{mg_1t}(\mu_3 y_2^{g_1-1}y_3-\bar{\mu_3}\bar{y_2}^{g_1-1}\bar{y_3}),\\
(\mu_3-\bar{\mu_3})'-m(\mu_3-\bar{\mu_3}) =& -\sigma_1 e^{mt}(\mu_1y_1-\bar{\mu_1}\bar{y_1})-\sigma_2 e^{mt}(\mu_2y_2-\bar{\mu_2}\bar{y_2})\\
&-\alpha_3(\mu_3-\bar{\mu_3})+\frac{2\alpha_3 e^{mt}}{K}(\mu_3y_3-\bar{\mu_3}\bar{y_3})\\
&+\beta_3(\mu_3-\bar{\mu_3})\\
&-\sigma_3 e^{mg_2t}(y_1^{g_2}-\bar{y_1}^{g_2})-\sigma_4 e^{mg_1t}(y_2^{g_1}-\bar{y_2}^{g_1})\\
&-2e^{2mt}(y_3-\bar{y_3}).
\end{aligned}
$$

Now, we multiply each equation by the left-hand side without the derivative and then integrate from 0 to a time T. We present next the result of doing this just for y_1 and μ_1 since the other variables have similar expressions:

$$
\begin{aligned}
&\frac{1}{2}(y_1-\bar{y_1})^2\Big|_0^T+m\int_0^T(y_1-\bar{y_1})^2dt\\
&\quad=\alpha_1\int_0^T(y_1-\bar{y_1})e^{mg_1t}(y_1y_2^{g_1}-\bar{y_1}\bar{y_2}^{g_1})dt\\
&\qquad-\alpha_1\int_0^T(y_1-\bar{y_1})e^{mg_1t}(y_1y_2^{g_1}u-\bar{y_1}\bar{y_2}^{g_1}\bar{u})dt\\
&\qquad-\beta_1\int_0^T(y_1-\bar{y_1})^2dt+\sigma_1\int_0^T(y_1-\bar{y_1})e^{mt}(y_1y_3-\bar{y_1}\bar{y_3})dt,\\
&\qquad-\frac{1}{2}(\mu_1-\bar{\mu_1})^2\Big|_0^T+m\int_0^T(\mu_1-\bar{\mu_1})^2dt=
\end{aligned}
$$

$$
\begin{aligned}
&\alpha_1 \int_0^T (\mu_1 - \bar{\mu_1}) e^{mg_1 t} (\mu_1 y_2^{g_1} - \bar{\mu_1} \bar{y_2}^{g_1}) dt \\
&- \alpha_1 \int_0^T (\mu_1 - \bar{\mu_1}) e^{mg_1 t} (\mu_1 y_2^{g_1} u - \bar{\mu_1} \bar{y_2}^{g_1} \bar{u}) dt \\
&- \beta_1 \int_0^T (\mu_1 - \bar{\mu_1})^2 dt + \sigma_1 \int_0^T (\mu_1 - \bar{\mu_1}) e^{mt} (\mu_1 y_3 - \bar{\mu_1} \bar{y_3}) dt \\
&+ \alpha_2 g_2 \int_0^T (\mu_1 - \bar{\mu_1}) e^{mg_2 t} (\mu_2 y_1^{g_2 - 1} y_2 - \bar{\mu_2} \bar{y_1}^{g_2 - 1} \bar{y_2}) dt \\
&+ \sigma_3 g_2 \int_0^T (\mu_1 - \bar{\mu_1}) e^{mg_2 t} (\mu_3 y_1^{g_2 - 1} y_3 - \bar{\mu_3} \bar{y_1}^{g_2 - 1} \bar{y_3}) dt.
\end{aligned}
$$

On the other hand, we also have:

$$
\begin{aligned}
\int_0^T (u - \bar{u})^2 dt = &\int_0^T \left(\max \left\{ 0, \min \left\{ 1, \frac{\alpha_1 e^{mg_1 t} y_1 y_2^{g_1} \mu_1}{2B} \right\} \right\} \right. \\
&\left. - \max \left\{ 0, \min \left\{ 1, \frac{\alpha_1 e^{mg_1 t} \bar{y}_1 \bar{y}_2^{g_1} \bar{\mu}_1}{2B} \right\} \right\} \right)^2 dt \\
\leq &\int_0^T \left(\frac{\alpha_1 e^{mg_1 t} y_1 y_2^{g_1} \mu_1}{2B} - \frac{\alpha_1 e^{mg_1 t} \bar{y}_1 \bar{y}_2^{g_1} \bar{\mu}_1}{2B} \right)^2 dt \\
\leq &\frac{\alpha_1}{2B} \int_0^T \left(y_1 y_2^{g_1} \mu_1 - \bar{y}_1 \bar{y}_2^{g_1} \bar{\mu_1} \right)^2 dt.
\end{aligned}
$$

Now, using that the function $f(y_1, y_2, \mu_1) = y_1 y_2^{g_1} \mu_1$ is locally Lipschitz, we can conclude that there exists a positive constant L such that:

$$
\begin{aligned}
&\frac{\alpha_1}{2B} \int_0^T \left(y_1 y_2^{g_1} \mu_1 - \bar{y}_1 \bar{y}_2^{g_1} \bar{\mu_1} \right)^2 dt \\
&\leq \frac{\alpha_1 L}{2B} \int_0^T \left((y_1 - \bar{y_1})^2 + (y_2 - \bar{y_2})^2 + (\mu_1 - \bar{\mu_1})^2 \right) dt.
\end{aligned}
$$

Another useful inequality is derived from using Lemma 6 two times successively and the locally Lipschitz condition for $f(y_2) = y_2^{g_1}$. Hence we have:

$$
|y_1 - \bar{y_1}|(y_1 y_2^{g_1} u - \bar{y_1} \bar{y_2}^{g_1} \bar{u}) \leq M_5((y_1 - \bar{y_1})^2 + (u - \bar{u})^2 + (y_2 - \bar{y_2})^2)
$$

for some constant $M_5 > 0$. Now, using the previous results and summing up the expression for the six variables we can get: Summing the above six equations and grouping terms we get:

$$
\left(m - L_{11} - L_{12} e^{mT} - L_{13} - L_{21} e^{mg_2 T} - L_{22} e^{mT} - L_{31} - L_{32} e^{mT} \right.
$$

$$-L_{33}e^{mg_2T} - L_{34} - L_{41} - L_{42} - L_{43}e^{mT} - L_{44}e^{mg_2T} - L_{45}e^{mg_2T} - L_{51} - L_{52}$$
$$- L_{53}e^{mg_2T} - L_{54}e^{mT} - L_{55} - L_{61}e^{mT} - L_{62}e^{mT} - L_{63} - L_{64}e^{mT} - L_{65}e^{mg_2T}$$
$$-L_{66}e^{2mT} - L_{67}\Big) \int_0^T \Big((y_1 - \bar{y_1})^2$$
$$+(y_2 - \bar{y_2})^2 + (y_3 - \bar{y_3})^2 + (\mu_1 - \bar{\mu_1})^2 + (\mu_2 - \bar{\mu_2})^2 + (\mu_3 - \bar{\mu_3})^2\Big)\, dt \leq 0.$$

This can be rewritten as:

$$\Big(m - C_1 - C_2e^{mT} - C_3e^{mg_2T} - C_4e^{2mT}\Big)$$
$$\int_0^T \Big((y_1 - \bar{y_1})^2 + (y_2 - \bar{y_2})^2 + (y_3 - \bar{y_3})^2$$
$$+(\mu_1 - \bar{\mu_1})^2 + (\mu_2 - \bar{\mu_2})^2 + (\mu_3 - \bar{\mu_3})^2\Big)\, dt \leq 0.$$

So if $m - C_1 - C_2e^{mT} - C_3e^{mg_2T} - C_4e^{2mT} > 0$ then $y_1 = \bar{y_1}$, $y_2 = \bar{y_2}$, $y_3 = \bar{y_3}$, $\mu_1 = \bar{\mu_1}$, $\mu_2 = \bar{\mu_2}$ and $\mu_3 = \bar{\mu_3}$, and therefore the OC solutions u and $\bar{u}$ are the same. □

References

Araujo A, Cook LM, Lynch CC, Basanta D (2014) An integrated computational model of the bone microenvironment in bone-metastatic prostate cancer. Cancer Res 74(9):2391–2401

Ayati BP, Edwards CM, Webb GF, Wikswo JP (2010) A mathematical model of bone remodeling dynamics for normal bone cell populations and myeloma bone disease. Biol Direct 5(1):28

Barker HE, Paget JT, Khan AA, Harrington KJ (2015) The tumour microenvironment after radiotherapy: mechanisms of resistance and recurrence. Nat Rev Cancer 15(7):409

Bara O, Djouadi SM, Day JD, Lenhart S (2017) Immune therapeutic strategies using optimal controls with L1- and L2- type objectives. Math Biosci 290:1339–1351

Brenner DJ (2008) The linear-quadratic model is an appropriate methodology for determining isoeffective doses at large doses per fraction. Semin Radiat Oncol 8(4):234–239

Chow E, van der Linden YM, Roos D, Hartsell WF, Hoskin P, Wu JSY, Wong RKS (2016) Single versus multiple fractions of repeat radiation for painful bone metastases: a randomised, controlled, non-inferiority trial. Lancet Oncol 15(2):164–171

Coelho RM, Lemos JM, Alho I, Valério D, Ferreira AR, Costa L, Vinga S (2016) Dynamic modeling of bone metastasis, microenvironment and therapy. J Theor Biol 391:1–12

De Pillis LG, Radunskaya A (2003) The dynamics of an optimally controlled tumor model: a case study. Math Comput Model 37(11):1221–1244

Dingli D, Chalub FACC, Santos FC, Van Segbroeck S, Pacheco JM (2009) Cancer phenotype as the outcome of an evolutionary game between normal and malignant cells. Br J Cancer 101(7):1130–1136

Farhat A, Jiang D, Cui D, Keller ET, Jackson TL (2017) An integrative model of prostate cancer interaction with the bone microenvironment. Math Biosci 294:1–14

Fister KR, Lenhart S, McNally JS (1998) Optimizing chemotherapy in an HIV model. Electron J Differ Equ 32:1–12

Fleming WH, Rishel RW (1975) Deterministic and stochastic optimal control. Springer, New York

Florencio-Silva R, Rodrigues G, Sasso-Cerri E, Simoes MJ, Cerri PS (2015) Biology of bone tissue: structure, function, and factors that influence bone cells. Biomed Res Int 2015:421746

Ganesh V, Chan S, Raman S, Chow R, Hoskin P, Lam H, Chow E (2017) A review of patterns of practice and clinical guidelines in the palliative radiation treatment of uncomplicated bone metastases. Radiother Oncol 124(1):38–44

Garzón-Alvaradob DA (2012) A mathematical model for describing the metastasis of cancer in bone tissue. Comput Methods Biomech Biomed Eng 15(4):333–346
Graham JM, Ayati BP, Ramakrishnan PS, Martin JA (2012) Towards a new spatial representation of bone remodeling. Math Biosci Eng 9(2):281–295
Jerez S, Chen B (2015) Stability analysis of a Komarova type model for the interactions of osteoblast and osteoclast cells during bone remodeling. Math Biosci 264:29–37
Jerez S, Camacho A (2018) Bone metastasis modeling based on the interactions between the BMU and tumor cells. J Comput App Math 330:866–876
Jerez S, Díaz-Infante S, Chen B (2018) Fluctuating periodic solutions and moment boundedness of a stochastic model for the bone remodeling process. Math Biosci 299:153–164
Juárez P, Fournier PG, Mohammad KS, McKenna RC, Davis HW, Peng XH, Guise TA (2017) Halofuginone inhibits TGF-β/BMP signaling and in combination with zoledronic acid enhances inhibition of breast cancer bone metastasis. Oncotarget 8(49):86447
Komarova SV, Smith RJ, Dixon SJ, Sims SM, Wahl LM (2003) Mathematical model predicts a critical role for osteoclast autocrine regulation in the control of bone remodeling. Bone 33(2):206–215
Kwakwa KA, Vanderburgh JP, Guelcher SA, Sterling JA (2017) Engineering 3D models of tumors and bone to understand tumor-induced bone disease and improve treatments. Curr Osteoporos Rep 15(4):247–254
Lemaire V, Tobin FL, Greller LD, Cho CR, Suva LR (2004) Modeling the interactions between osteoblast and osteoclast activities in bone remodeling. J Theor Biol 229(3):293–309
Lemos JM, Caiado DV, Coelho R, Vinga S (2016) Optimal and receding horizon control of tumor growth in myeloma bone disease. Biomed Signal Process 24:128–134
Lenhart S, Workman JT (2007) Optimal control applied to biological models. Chapman & Hall/CRC, Boca Raton
Lipton A, Fizazi K, Stopeck AT, Henry DH, Smith MR (2016) Effect of denosumab versus zoledronic acid in preventing skeletal-related events in patients with bone metastases by baseline characteristics. Eur J Cancer 53:75–83
Lukes DL (1982) Differential equations: classical to controlled. Academic Press, New York
Lutz S, Balboni T, Jones J, Lo S, Petit J, Rich SE, Wong R, Hahn C (2017) Palliative radiation therapy for bone metastases: update of an ASTRO evidence-based guideline. Pract Radiat Oncol 7(1):4–12
Massagué J, Obenauf AC (2016) Metastatic colonization by circulating tumour cells. Nature 529(7586):298–306
McAsey M, Mou L, Han W (2012) Convergence of the forward-backward sweep method in optimal control. Comput Optim Appl 53(1):207–226
Mundy GR (2002) Metastasis to bone: causes, consequences and therapeutic opportunities. Nat Rev Cancer 2(8):584–593
Oest ME, Franken V, Kuchera T, Strauss J, Damron TA (2015) Longterm loss of osteoclasts and unopposed cortical mineral apposition following limited field irradiation. J Orthop Res 33(3):334–342
Ottewell PD (2016) The role of osteoblasts in bone metastasis. J Bone Oncol 5(3):124–127
Paget S (1889) The distribution of secondary growths in cancer of the breast. Lancet 133(3421):571–573
Penninger CL, Patel NM, Niebur GL, Tovar A, Renauda JE (2008) A fully anisotropic hierarchical hybrid cellular automaton algorithm to simulate bone remodeling. Mech Res Commun 35(1–2):32–42
Pivonka P, Zimak J, Smith DW, Gardiner BS, Dunstan CR, Sims NA, Martin TJ, Mundy GR (2008) Model structure and control of bone remodeling: a theoretical study. Bone 43(2):249–263
Pontryagin LS, Boltyanskiĭ VG, Gamkrelidze RV, Mischenko EF (1962) The mathematical theory of optimal processes. Wiley, New York
Ross DS, Mehta K, Cabal A (2017) Mathematical model of bone remodeling captures the antiresorptive and anabolic actions of various therapies. Bull Math Biol 79(1):117–142
Ryser MD, Qu Y, Komarova SV (2012) Osteoprotegerin in bone metastases: mathematical solution to the puzzle. PLoS Comput Biol 8(10):e1002703
Savageau MA (1988) Introduction to S-systems and the underlying power-law formalism. Math Comput Model 11:546–551
Stephenson B, Lanzas C, Lenhart S, Day J (2017) Optimal control of vaccination rate in an epidemiological model of *Clostridium difficile* transmission. J Math Biol 75(6–7):1693–1713
Swan GW (1990) Role of optimal control theory in cancer chemotherapy. Math Biosci 101(2):237–284
Theriault RL, Theriault RL (2012) Biology of bone metastases. Cancer Control 19(2):92–101

Tovar A (2004) Bone remodeling as a hybrid cellular automaton optimization process. Ph.D dissertation, University of Notre Dame, Indiana

Vakaet LAM-L, Boterberg T (2004) Pain control by ionizing radiation of bone metastasis. Int J Dev Biol 48(5–6):599–606

Van Scoy GK, George EL, Asantewaa FO, Kerns L, Saunders MM, Prieto-Langarica A (2017) A cellular automata model of bone formation. Math Biosci 286:58–64

Wang Y, Pivonka P, Buenzli PR, Smith DW, Dunstan CR (2011) Computational modeling of interactions between multiple myeloma and the bone microenvironment. PLoS One 6(11):e27494

Warman P, Kaznatcheev A, Araujo A, Lynch C, Basanta D (2018) Fractionated follow-up chemotherapy delays the onset of resistance in bone metastatic prostate cancer. Games 9(2):19

Zhang J, Qiu X, Xi K, Hu W, Pei H, Nie J, Zhou G (2018) Therapeutic ionizing radiation induced bone loss: a review of in vivo and in vitro findings. Connect Tissue Res 29:1–14